Roles and mechanisms of action of *HNF-4α* in the hepatic differentiation of WB-F344 cells

YUMENG SHI[1*], DEHUA ZHOU[2*], BINGYI WANG[2], DEREN ZHOU[2] and BAOMIN SHI[2]

[1]Cheeloo College of Medicine, Shandong University, Jinan, Shandong 250012;
[2]Department of General Surgery, Tongji Hospital, Tongji University Medical School, Shanghai 200065, P.R. China

Received May 10, 2018; Accepted November 26, 2018

DOI: 10.3892/ijmm.2018.4010

Abstract. Hepatocyte nuclear factor 4 α (*HNF-4α*) is a nuclear receptor and mediates hepatic genes. WB-F344 liver epithelial cells can differentiate into hepatocytes. The present study aimed to examine the roles and mechanisms of action of *HNF-4α* on the hepatic differentiation of WB-F344 cells. WB-F344 cells were divided into a normal cell group (WB-F344), empty vector group (PLKO), and gene silencing group (PLKO-SH). The expression levels of *HNF-4α* were measured using reverse transcription-quantitative polymerase chain reaction analysis. Proliferation of the cells was determined using a Cell Counting kit-8 assay. Based on western blot analysis, the protein levels of α-fetoprotein (AFP), albumin (ALB) and cytokeratin 19 (CK19) were determined. The positive cell rates of the three groups were assessed using periodic acid-Schiff (PAS) staining. Following construction of an RNA-sequencing library, differentially expressed genes (DEGs) between the *HNF-4α*-silenced and normal samples were screened using the limma package and enrichment analysis was conducted using the DAVID tool. Protein-protein interaction (PPI) and microRNA-targeted regulatory networks were constructed in Cytoscape software. The PLKO-SH group exhibited a lower mRNA level of *HNF-4α*, higher protein level of AFP, lower protein levels of ALB and CK19, increased cell proliferation, and a lower PAS-positive cell rate. The *HNF-4α*-silenced and normal samples differed in 499 DEGs. In the PPI network, matrix metallopeptidase 9 (MMP9), early growth response 1 (EGR1), SMAD family member 2 (SMAD2), and RAS-related C3 botulinum substrate 2 (RAC2) were key nodes. *HNF-4α* may promote the differentiation of WB-F344 cells into hepatocytes by targeting *MMP9*, *EGR1*, *SMAD2* and *RAC2*.

Correspondence to: Dr Baomin Shi, Department of General Surgery, Tongji Hospital, Tongji University Medical School, 389 Xincun Road, Shanghai 200065, P.R. China
E-mail: baominsph@163.com

*Contributed equally

Key words: hepatocyte nuclear factor 4 α, WB-F344 cells, hepatocyte differentiation, differential expression of genes, protein interaction network

Introduction

Hepatocyte nuclear factor 4 α (*HNF-4α*; also known an nuclear receptor subfamily 2 group A member 1) is a nuclear receptor and a major mediator of liver-specific gene expression (1). *HNF-1α* acts as a transcription factor that mediates hepatic genes, and HNF-4α protein can regulate the expression of *HNF-1α* (2,3). *HNF-4α* is critical for the development of the kidney, liver and intestines (4). By regulating *HNF-4α*, nuclear receptor subfamily 1 group H member 3 can promote the hepatic differentiation of hepatocyte-like cells (5). *HNF-4α* also influences the expression and synthesis of sex-hormone-binding globulin, a key glycoprotein that is mainly produced by the liver (6,7). WB-F344 cells, which originate from monoclonal epithelial cells of the rat liver, are analogous to liver precursor cells (8,9). WB-F344 cells acquire some phenotypic and functional characteristics of hepatocytes when they are transplanted into the liver (10,11). However, the roles and mechanisms of action of *HNF-4α* on WB-F344 cell differentiation remain to be fully elucidated.

Bone morphogenetic protein 4 (*BMP4*), belongs to the transforming growth factor-β (*TGF-β*) superfamily. It can promote the differentiation of WB-F344 cells to the hepatocyte lineage (12). WB-F344 cells cultured on Matrigel can differentiate to biliary cells, during which the expression of Ras homolog family member A (*RhoA*) is increased and the RhoA-Rho-associated protein kinase-stress fiber system is essential (10,13). The canonical Wnt signaling pathway has a positive effect on self-renewal and proliferation of rat WB-F344 cells (14). Through suppression of the Hes family bHLH transcription factor 1 signaling pathway, matrine (an alkaloid constituent of plants in the genus *Sophora*) can stimulate the differentiation of WB-F344 cells into hepatocytes (11).

Although the above studies have reported that several genes are correlated with the hepatic differentiation of WB-F344 cells, the mechanism of action of *HNF-4α* on WB-F344 cell differentiation remains to be elucidated. To address this gap in knowledge, the present study experimentally investigated the roles of *HNF-4α* on WB-F344 cells and examined the potential

mechanisms of action using comprehensive bioinformatics analyses.

Materials and methods

Vector construction. The WB-F344 cells were purchased from Shanghai Bioleaf Biotech Co., Ltd. (Shanghai, China). Full-length *HNF-4α* was synthesized from the cDNA of WB-F344 cells using the forward primer 5'-CCGGGCTGC AGATCGATGATAATGATCAAGAGATCATTATCATCG ATCTGCAGCTTTTTGGATCC-3' and the reverse primer 3'-CGACGTCTAGCTACTATTACTAGTTCTCTAGTAATA GTAGCTAGACGTCGAAAAACCTAGGTTAA-5'. The *HNF-4α* fragment was inserted into the *Age*I and *Eco*RI sites of the pLKO.1-EGFP-Puro vector (Takara Bio, Inc., Otsu, Japan) to construct the recombinant plasmid. The recombinant plasmids were amplified, purified, and finally verified by agarose gel electrophoresis and DNA sequencing.

Virus packaging and the identification of stably transfected WB-F344 cells. The cells were digested in pancreatin and plated in culture dishes (60x15 mm, $2.5x10^6$ cells/dish). Following growth to 80% confluence in Dulbecco's modified Eagle medium (DMEM; Gibco; Thermo Fisher Scientific, Inc., Waltham, MA, USA) in a humidified 5% CO_2 incubator (Thermo Fisher Scientific, Inc.), the cells were used for transfection experiments. Into tube 1 4 μg pCDH plasmid/recombinant plasmid, 3 μg psPAX2, and 2 μg pMD2.G were dissolved in 600 μl opti-MEM and were placed at room temperature for 5 min following gentle mixing. In tube 2, 600 μl serum-free medium was mixed with 20 μl Lipofectamine 2000 (Thermo Fisher Scientific, Inc.) and left at room temperature for 5 min. The solutions in tubes 1 and 2 were mixed again and left for 20 min. The mixture was cultured in a humidified 5% CO_2 incubator (Thermo Fisher Scientific, Inc.) at 37˚C and the medium was replaced with complete medium after 6 h. Following culture for 48 h, the supernatant was collected in a 15-ml centrifuge tube and maintained at 4˚C. Subsequently, the supernatant was added to 4 ml complete medium and cultured in an incubator for 24 h. The supernatant was transferred into a 15-ml centrifuge tube and mixed with the virus suspension collected the previous day. The virus suspension was concentrated.

The cells were spread on medium in 12-well plates and cultured at 37˚C overnight. The original medium was replaced with a half-volume of fresh medium, and the virus solution was mixed with the cells. Following infection at 37˚C for 4 h, the medium was supplemented to the normal volume. The medium containing the virus was replaced with fresh medium on the second day following infection, and cultivation of the cells was continued at 37˚C. Following infection for 48 h, fluorescence microscopy examination (Olympus Corporation, Tokyo, Japan) was used to detect viruses harboring the green fluorescent protein (*GFP*) reporter gene to observe the expression efficiency of *GFP*. For the viruses carrying the puromycin resistance gene, the medium was replaced with fresh medium containing an appropriate concentration of puromycin to identify the stably transfected cells.

Reverse transcription-quantitative polymerase chain reaction (RT-qPCR) analysis. Total RNA was extracted using RNAiso Plus (Takara Bio, Inc.) according to the manufacturer's protocol. The density and purity of RNA were measured by spectrophotometry (Merinton, Beijing, China). Total RNA was reverse transcribed into cDNA using PrimeScript™ RT Master mix (Takara Bio, Inc.). The primer sequences for the RT-qPCR experiments were produced by Sangon Biotech Co., Ltd. (Shanghai, China) and are listed in Table I. Using the SYBR Green master mix kit (Applied Biosystems; Thermo Fisher Scientific, Inc.), RT-qPCR amplification was performed using the following amplification system: 10 μl SYBR Premix Ex Taq (2X), 2 μl cDNA template, 0.4 μl forward primer, 0.4 μl reverse primer, and RNase-free distilled water up to 20 μl. The reaction processes were as follows: 95˚C for 10 min; 95˚C for 15 sec and 60˚C for 1 min for 40 cycles. The subsequent melting processes were 95˚C for 15 sec, 60˚C for 1 min, and 95˚C for 15 sec. All samples had three repeats, with actin as the reference gene. The relative gene expression was calculated using the $2^{-\Delta\Delta Cq}$ method (15).

Table I. Primer sequences used for reverse transcription-quantitative polymerase chain reaction analysis.

Primer name	Primer sequence (5'-3')
HNF-4α-F	CAGTATGACTCTCGGGGTCGTTTTG
HNF-4α-R	CCATGCCAAAGAGCTTGATGAACTG
Actin-F	CCCATCTATGAGGGTTACGC
Actin-R	TTTAATGTCACGCGATTTC

HNF-4α, hepatocyte nuclear factor 4α; F, forward; R, reverse.

Cell Counting kit-8 (CCK-8) assay. Following culture of the cells for 12, 24 and 48 h, they were digested to prepare the cell suspension ($1.5x10^5$ cells/ml). Subsequently, 100 μl of each cell suspension was inoculated into 96-well plates (ABI; Thermo Fisher Scientific, Inc.; $1.5x10^4$ cells/well). The cells were divided into the WB-F344 normal cell group (WB-F344), empty vector control group (PLKO), and gene silencing group (PLKO-SH). Each group had three replicate wells. The 96-well plates were cultured in an incubator (Thermo Fisher Scientific, Inc.) for 0, 24 and 48 h, following which 10 ml CCK-8 solution (Tongren, Shanghai, China) was added. The plates were incubated in an incubator (Thermo Fisher Scientific, Inc.) for 1.5 h. Using a microplate reader (BioTek Instruments, Inc., Winooski, VT, USA), the absorbance of each well at an optical density of 450 nm was detected. The absorbance value with time was plotted.

Western blot analysis. The cells were lysed in radioimmunoprecipitation assay lysis buffer (Beyotime Institute of Biotechnology, Shanghai, China) on ice for 30 min. The lysates were centrifuged at low temperature (4˚C, 12,000 x g, 15 min) and the supernatants were transferred to sterile centrifuge tubes. Protein concentrations were measured using a bicinchoninic acid protein assay kit (Sangon Biotech Co., Ltd., Shanghai, China). The cell lysates (15 μl each hole) were used for SDS-PAGE on 10% polyacrylamide and resolved proteins were transferred onto a polyvinylidene

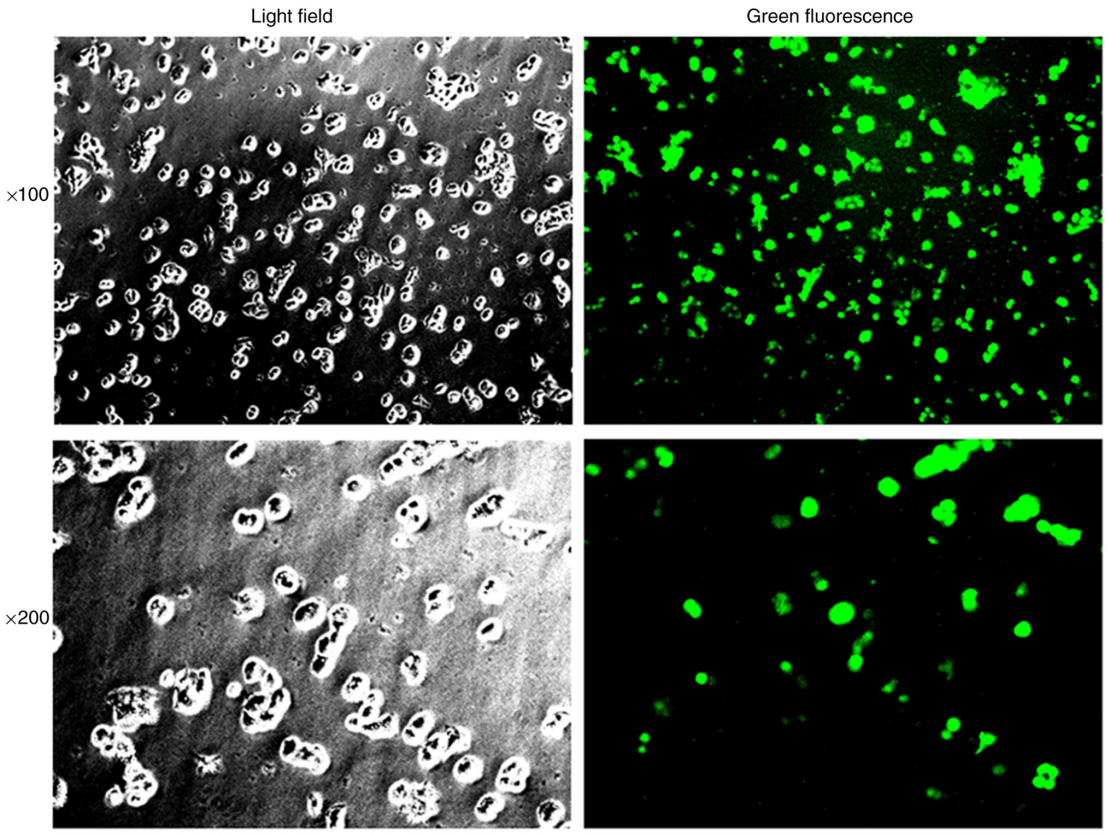

Figure 1. WB-F344 cells transfected with a packaged virus. Green represents the cells expressing green fluorescent protein.

fluoride membrane (Merck KGaA, Darmstadt, Germany). The membranes were blocked in 5% skim milk (0.75 g milk powder in 15 ml phosphate buffered saline) at 37˚C for 1-2 h, following which they were incubated at 4˚C overnight with the primary antibodies (ProteinTech Group, Inc., Chicago, IL, USA). The primary antibodies included albumin (ALB; cat. no. 16475-1-AP; 1:2,000), α-fetoprotein (AFP; cat. no. 14550-1-AP; 1:1,000), and cytokeratin 19 (CK-19; cat. no. 10712-1-AP; 1:500). The membranes were incubated with horseradish peroxidase-labeled goat anti-rabbit secondary antibody (1:1,000; Beyotime Institute of Biotechnology; cat. no. A0208) at 37˚C for 2 h. The blots were developed using ECL detection reagent, and a gel imaging analysis system (Bio-Rad Laboratories Inc., Richmond, CA, USA) was utilized to detect the results.

Periodic acid-Schiff (PAS) staining. The slides of cells were prepared and PAS staining was performed using PAS/Glycogen Stain kit (Nanjing Jiancheng Bioengineering Institute, Nanjing, China). The cells were incubated with reagent 1 at room temperature for 10 min and washed with tap water for 3-5 min. They were then incubated with reagent 2 at room temperature for 10-15 min and rinsed for 30-60 sec. Counterstaining was performed with reagent 3 for 20-30 sec. Following rinsing in tap water, the slides were covered and observed using an inverted microscope (Olympus Corporation).

RNA extraction and RNA-seq library construction. Total RNA of the three *HNF-4α*-silenced WB-F344 cells and three normal WB-F344 cells were extracted using TRIzol reagent (Takara Bio, Inc.) and measured using a Nanodrop spectrophotometer. An RNA-seq library was constructed with sequencing performed separately using a NEBNext® Ultra™ RNA Library Prep kit (New England Biolabs, Inc., Ipswich, MA, USA) and a Hiseq 4000 system, (PE150; Illumina, Inc., San Diego, CA, USA). The sequencing data were deposited into the Sequence Read Archive database (http://www.ncbi.nlm.nih.gov/sra/), under accession no. SRP135721.

Differential expression and enrichment analyses. To filter out unreliable bases and reads, the raw data were quality control analyzed. The barcode and adaptor sequences were removed from the reads. Subsequently, any reads with >5% of N content were eliminated. Bases with continuous quality <10 were eliminated from the 5' or 3' end. The low-quality reads, in which the number of the bases with quality <20 exceeded 20%, and the short reads, which had a length <30 nt, were filtered out. These steps allowed the acquisition of clean reads of the six samples. Using Tophat software (version 2.0.8, with default parameters; http://www.ccb.jhu.edu/software/tophat/) (16), the clear reads were mapped to the rat reference genome downloaded from the Ensembl database (version 6.0; http://www.ensembl.org/) (17). Based on the rat gene annotation information in the Ensembl database, the raw reads corresponding to each gene were obtained using the Htseq-count tool (version 0.6.1p2; http://www- huber.embl.de/users/anders/HTSeq/doc/count.html) (18).

Using trimmed mean of M values normalization in the R package edgeR (http://www.bioconductor.org/packages/release/bioc/html/edgeR.html) (19,20), the

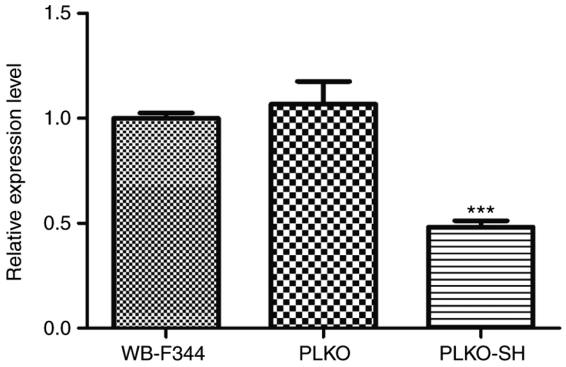

Figure 2. Relative mRNA expression levels of hepatocyte nuclear factor 4α in the normal WB-F344, PLKO and PLKO-SH groups. ***P<0.0001, compared with the WB-F344 and PLKO groups. WB-F344, normal cell group; PLKO, empty vector control group; PLKO-SH, gene silencing group.

read count data of gene expression were preprocessed. Subsequently, the preprocessed data were converted into gene expression matrices using the voom method (21) in the R package limma (http://www.bioconductor.org/packages/release/bioc/html/limma.html) (22). Differential expression analysis was performed using the linear model method in the limma package (22) and the significant P-values were calculated via moderated t-statistics (23). Differentially expressed genes (DEGs) were defined as genes with P<0.05 and $|\log_2$fold change (FC)$|\geq 0.58$. Using the DAVID tool (version 6.8, https://david.ncifcrf.gov/) (24). Gene Ontology (GO; http://www.geneontology.org) functional terms (25) and Kyoto Encyclopedia of Genes and Genomes (https://www.genome.jp/kegg/pathway.html) pathways (26) were enriched for the DEGs. A count of genes in each term ≥2 and P<0.05 were taken as the thresholds for selecting significant results.

Protein-protein interaction (PPI) network and microRNA (miRNA)-target regulatory network analyses. Using the STRING database (version 10.0, https://string-db.org) (27), the interactions among the proteins encoded by the DEGs were predicted. The parameter PPI score was set at 0.4. The PPI network was constructed based on Cytoscape software (version 3.4.0, http://www.cytoscape.org) (28). Using the CytoNCA plug-in (http://apps.cytoscape.org/apps/cytonca) (29) in the software, the importance of the network nodes were analyzed combined with the Degree centrality (DC) (30), Betweenness centrality (BC) (31), and Closeness centrality (CC) (32). Nodes with higher scores were considered key nodes in the PPI network.

Based on the Webgestalt tool (http://www.webgestalt.org) (33), miRNAs targeting the PPI network nodes were predicted. P<0.05 and a count of target genes ≥4 were defined as the thresholds. Finally, the miRNA-target regulatory network was visualized in Cytoscape software (28).

Statistical analysis. Based on GraphPad Prism software (version 5.0; GraphPad Software, Inc., San Diego, CA, USA), statistical analysis was performed using one-way analysis of variance with a two-tailed t-test and Bonferroni post hoc test. All data are presented as the mean ± standard error of the mean. P<0.05 was considered to indicate a statistically significant difference.

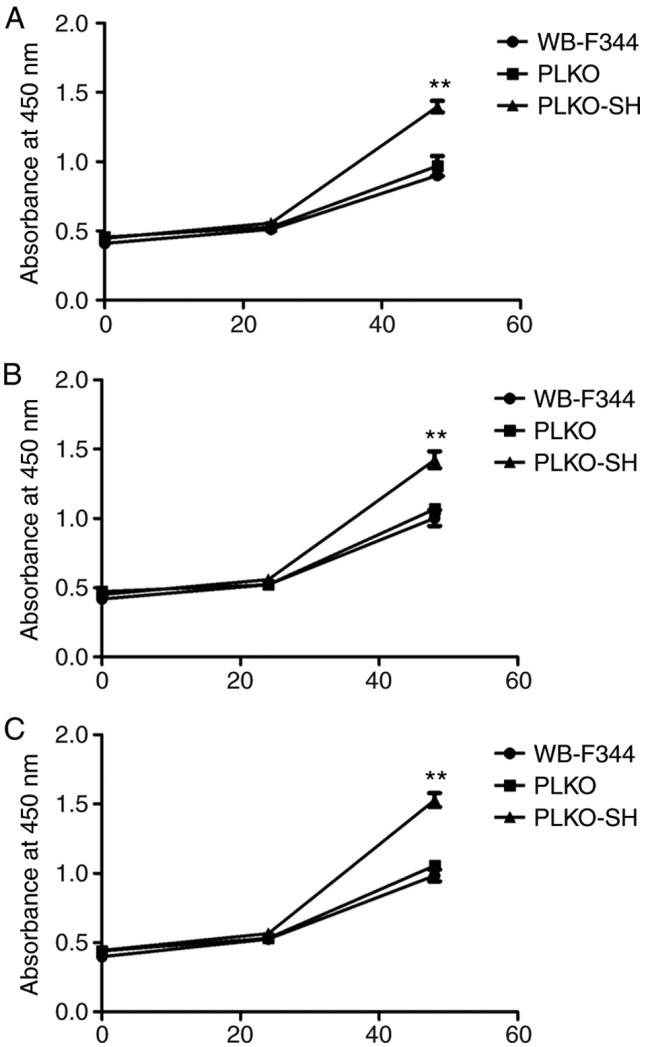

Figure 3. Proliferation of cells. Proliferation of different groups of cells following culturing for (A) 12 h, (B) 24 h and (C) 48 h. **P<0.01, compared with the WB-F344 and PLKO groups. WB-F344, normal cell group; PLKO, empty vector control group; PLKO-SH, gene silencing group.

Results

HNF-4α promotes the differentiation of WB-F344 cells into hepatocytes. Following transfection of the WB-F344 cells with the packaged virus, >95% of the cells expressed GFP protein (Fig. 1). This infection efficiency of >95% indicated that the stably transfected WB-F344 cells were suitable for used in subsequent experiments. Compared with the WB-F344 and PLKO groups, *HNF-4α* was significantly downregulated in the PLKO-SH group (P<0.0001, Fig. 2). The CCK-8 assay indicated that the proliferation of cells in the PLKO-SH group was increased relative to those in the WB-F344 and PLKO groups (Fig. 3A-C). Cells in the PLKO-SH group exhibited higher protein levels of AFP and lower protein levels of ALB and CK19 compared with cells in the WB-F344 and PLKO groups (Fig. 4A-C). PAS staining indicated that the rate of positive cells in the PLKO-SH group was lower than the rate in the WB-F344

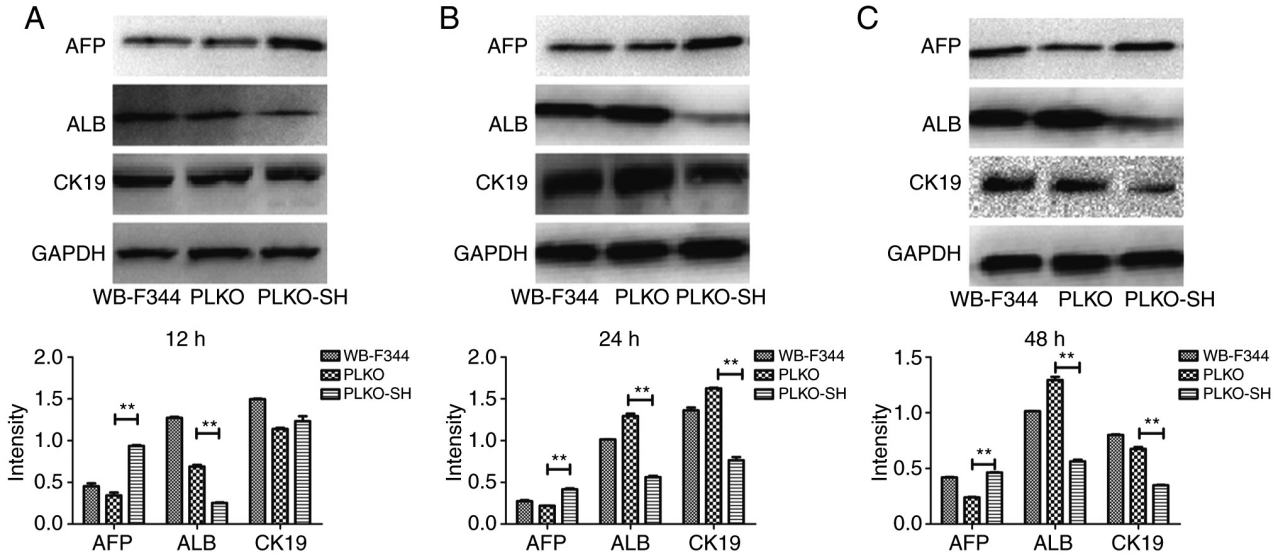

Figure 4. Protein expression levels of AFP, ALB, CK19 and GAPDH. Protein levels were determined in different groups of cells following culture for (A) 12 h, (B) 24 h and (C) 48 h. **P<0.01, compared with the WB-F344 and PLKO groups. WB-F344, normal cell group; PLKO, empty vector control group; PLKO-SH, gene silencing group; AFP, α-fetoprotein; ALB, albumin; CK19, cytokeratin 19; GAPDH, glyceraldehyde-3-phosphate dehydrogenase.

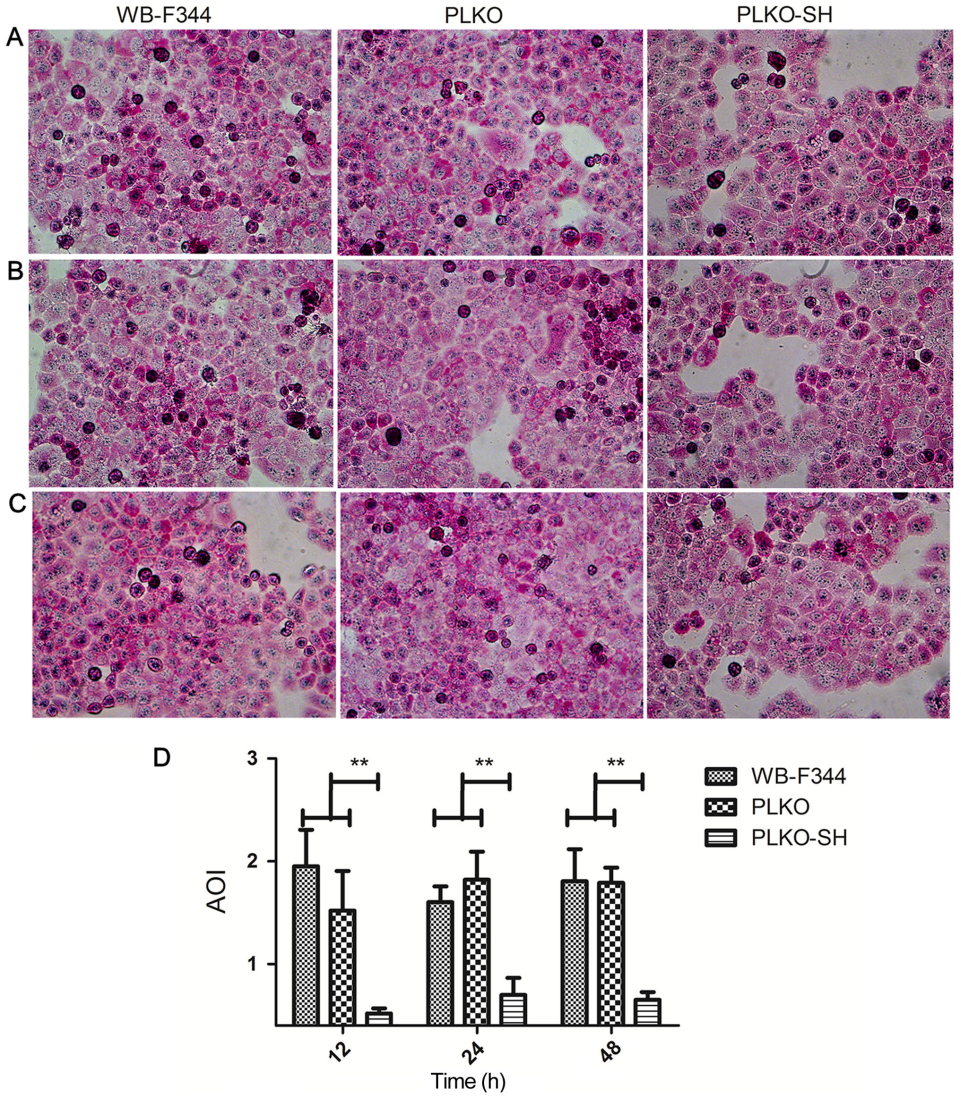

Figure 5. Periodic acid-Schiff staining to identify mature hepatocytes. Images of staining (magnification, x100) of different groups following culture for (A) 12 h, (B) 24 h and (C) 48 h; (D) corresponding column diagram. **P<0.01, compared with the WB-F344 and PLKO groups. WB-F344, normal cell group; PLKO, empty vector control group; PLKO-SH, gene silencing group; AIO, average optical density.

Table II. Top five GO functional terms and KEGG pathways enriched for the upregulated and downregulated genes.

A, Upregulated genes

Category	Term	P-value	Gene
GO	GO:0006955~immune response	5.24E-04	*MICB, RT1-M3-1, TNFSF13, CX3CL1, RT1-S3, SECTM1B, ZFR2, CXCL10, RT1-A2, TNFRSF9, MCPT8L2, OAS1A, OAS1F, OAS1G*
GO	GO:0042493~response to drug	7.27E-04	*EGR1, TXNIP, SNCG, TSPO, APOBEC1, PDXK, ASS1, PGF, MMP9, GSTT1, FOSB, MMP13, LCN2, ALDH1A1, HDAC5, ARG1, HSD11B2, FABP4, CAR9*
GO	GO:0071222~cellular response to lipopolysaccharide	8.47E-04	*LCN2, HDAC5, ARG1, TSPO, ASS1, NR1D1, MMP9, CD300LB, ENTPD2, CXCL10*
GO	GO:0051607~defense response to virus	2.30E-03	*OASL, APOBEC1, OAS1A, IL33, OAS1F, OAS1G, ISG20, CXCL10*
GO	GO:0032753~positive regulation of interleukin-4 production	2.85E-03	*IL20RB, RT1-S3, IL33, LGALS9*
PATHWAY	rno00480: Glutathione metabolism	1.20E-02	*GGT6, GSTT1, GGT1, GSTT2, GSTM7*
PATHWAY	rno05204: Chemical carcinogenesis	1.30E-02	*SULT1A1, LOC688778, HSD11B1, GSTT1, GSTT2, GSTM7*
PATHWAY	rno00980: Metabolism of xenobiotics by cytochrome P450	2.26E-02	*LOC688778, HSD11B1, GSTT1, GSTT2, GSTM7*
PATHWAY	rno04670: Leukocyte transendothelial migration	3.77E-02	*CLDN8, CLDN9, RAC2, MMP9, CLDN2, CLDN23*
PATHWAY	rno04142: Lysosome	4.62E-02	*CD68, AP1S2, NAGA, MCPT8L2, AP3B2, CTSE*

B, Downregulated genes

Category	Term	P-value	Gene
GO	GO:0001525~angiogenesis	1.61E-04	*HOXB3, NRCAM, WARS, FGF9, NOS3, MCAM, FGF1, EIF2AK3, UBP1*
GO	GO:0030968~endoplasmic reticulum unfolded protein response	6.62E-03	*ATF3, PPP1R15A, EIF2AK3, SERP1*
GO	GO:0070848~response to growth factor	1.31E-02	*SFTPC, SKIL, ANXA3*
GO	GO:1902010~negative regulation of translation in response to endoplasmic reticulum stress	1.66E-02	*SESN2, EIF2AK3*
GO	GO:0060734~regulation of endoplasmic reticulum stress-induced eIF2α phosphorylation	1.66E-02	*PPP1R15A, EIF2AK3*
PATHWAY	rno04141:Protein processing in endoplasmic reticulum	1.21E-02	*PLAA, LMAN1L, HYOU1, HSPA5, PPP1R15A, EIF2AK3*
PATHWAY	rno03008:Ribosome biogenesis in eukaryotes	3.55E-02	*GTPBP4, UTP14A, MDN1, GNL3*

GO, Gene Ontology; KEGG Kyoto, Kyoto Encyclopedia of Genes and Genomes.

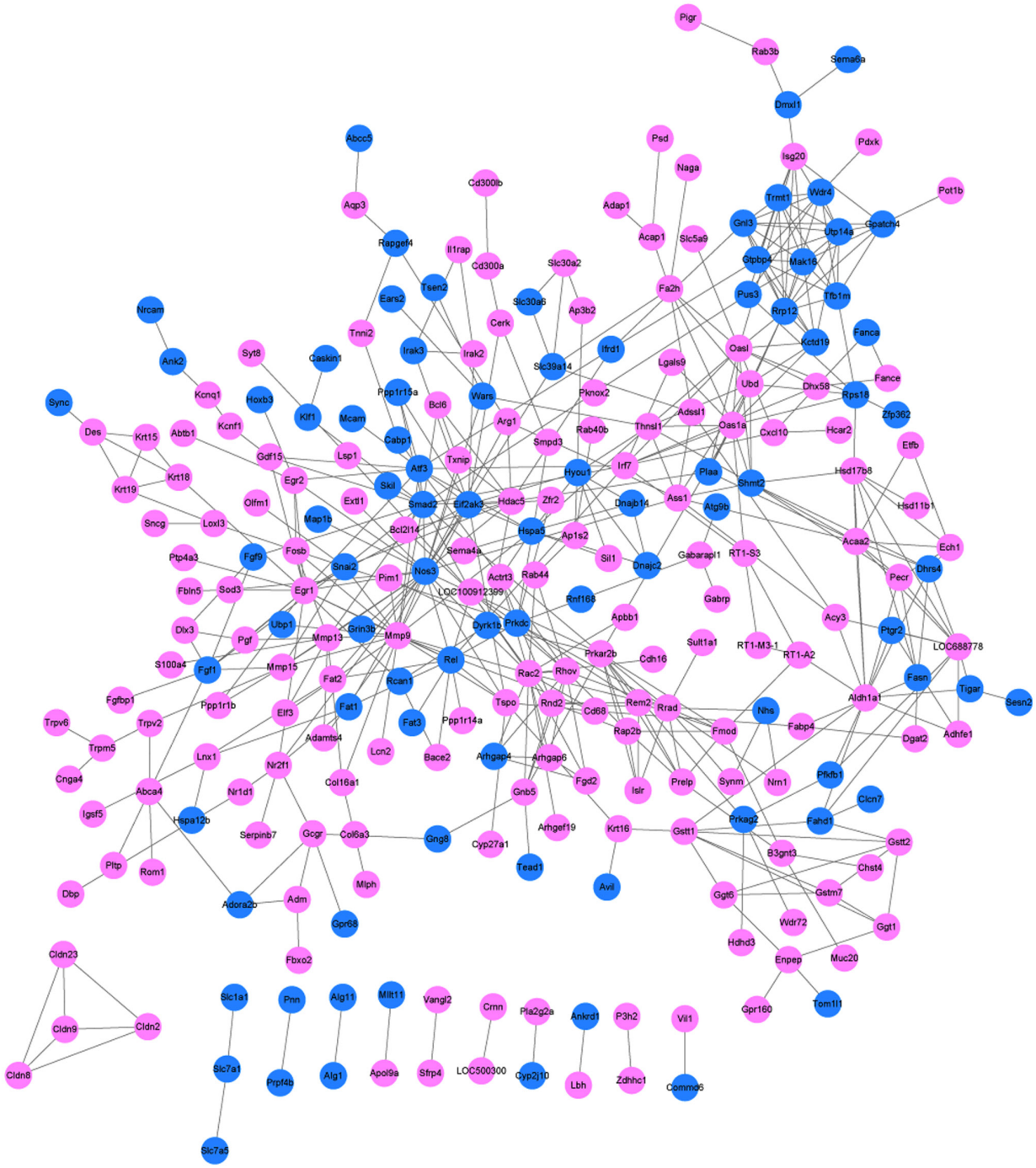

Figure 6. Protein-protein interaction network. Pink and blue circles represent upregulated genes and downregulated genes, respectively. Lines between nodes represent interactions.

and PLKO groups (Fig. 5A-D). These results demonstrated that *HNF-4α* contributed to the hepatocyte differentiation of WB-F344 cells.

Differential expression and enrichment analyses. There were 499 DEGs (305 upregulated and 194 downregulated) in the *HNF-4α*-silenced samples compared with the normal samples. The top five terms enriched for the upregulated genes and the downregulated genes are presented in Table IIA and B, respectively. The upregulated genes were mainly involved in response to drug (GO term) and chemical carcinogenesis (pathway). The downregulated genes were implicated in angiogenesis (GO term) and protein processing in the endoplasmic reticulum (pathway).

PPI network and miRNA-target regulatory network analyses. The PPI network had 255 nodes and 485 edges (Fig. 6). According to the BC, CC and DC scores, matrix metallopeptidase 9 (MMP9), early growth response 1 (EGR1), SMAD family member 2 (SMAD2), and RAS-related C3 botulinum substrate 2 (RAC2) were among the top 15 nodes (Table III). Enrichment analysis for the nine key nodes indicated that *RAC2*, *MMP9* and *SMAD2* were enriched in pathways in cancer (Table IV). A total

of 55 miRNAs targeting the PPI network nodes were obtained (Table V), which were used for constructing the miRNA-target regulatory network (Fig. 7).

Discussion

The PLKO-SH group exhibited a lower mRNA level of *HNF-4α*, increased cell proliferation, and lower a PAS-positive cell rate compared with the WB-F344 and PLKO groups. The cells in the PLKO-SH group had lower protein levels of ALB and CK19 compared with the cells in the WB-F344 and PLKO groups, indicating that the number of mature liver cells in the liver stem cells was decreased. Although the protein level of AFP, a differentiated hepatocyte marker, was not reduced in the PLKO-SH group, the WB-F344 cell was considered a suitable cell line for examining hepatocyte differentiation. A total of 499 DEGs (305 upregulated and 194 downregulated) between the *HNF-4α*-silenced samples and normal samples were identified. Based on the BC, CC and DC scores, MMP9, EGR1, SMAD2 and RAC2 were selected as the key nodes in the PPI network. Furthermore, 55 miRNAs were predicted for the PPI network nodes and used for constructing the miRNA-target regulatory network.

HNF-4α is critical in the transdifferentiation process of hematopoietic cells into hepatocytes (34). As an orphan nuclear receptor, *HNF-4α* is important in hepatic differentiation through the regulation of hepatocyte marker genes (35,36). A previous study demonstrated that *HNF-4α*, Snail, *miR-200*, and *miR-34a* are epistatic elements that regulate the maintenance and differentiation of hepatic stem cells (37). *HNF-4α* functions in hepatocyte differentiation and can suppress hepatocyte proliferation by inhibiting pro-mitogenic genes (38). These observations support the hypothesis that *HNF-4α* stimulates the hepatic differentiation of WB-F344 cells.

Activated *MMPs* control hepatic matrix remodeling, which helps to mediate the environment surrounding hepatocytes in the processes of liver regeneration (39,40). The *MMP* activation cascade and the positive feedback loop of *MMP9* contribute to the transdifferentiation of hepatic stellate cells induced by interleukin 1, indicating that *MMPs* are involved in liver injury and repair (41,42). By regulating the mesenchymal-to-epithelial transition (MET) process, *EGR1* stimulates the hepatic differentiation of bone marrow-derived mesenchymal stem cells (43). *EGR1*, which is a key mediator of liver fibrosis-associated genes, is regulated by a feedback loop between *HNF-4α* and small heterodimer partner (44). Therefore, *MMP9* and *EGR1* may be targets of *HNF-4α* during the hepatic differentiation of WB-F344 cells.

SMAD2 inhibits the growth and dedifferentiation of hepatocytes through a TGF-β signaling-independent pathway (45). The cyclin D1-SMAD2/3-SMAD4 signaling pathway contributes to the self-renewal of liver cancer stem cells, and TGF-β/SMAD inhibitor can induce liver cancer stem cell differentiation (46). *RAC1* is correlated with actin polymerization, and its inhibition can promote MET and enhance the differentiation of mesenchymal stromal cells toward hepatocytes (47). These observations indicate that *HNF-4α* may also promote the differentiation of WB-F344 cells into hepatocytes by targeting *SMAD2* and *RAC2*.

Table III. Top 15 protein-protein interaction network nodes according to Degree centrality, Betweenness centrality, and Closeness centrality.

Gene	Degree
Degree centrality	
Nos3	24.00
Mmp9	21.00
Egr1	17.00
Smad2	16.00
Rac2	15.00
Oasl	13.00
Rrp12	13.00
Rrad	12.00
Prkar2b	12.00
Rel	12.00
Oas1a	12.00
Aldh1a1	12.00
Eif2ak3	12.00
Atf3	11.00
Prkdc	10.00
Betweenness centrality	
Nos3	15,488.65
Mmp9	6,738.23
Prkar2b	6,486.67
Egr1	5,810.34
Smad2	5,786.24
Rac2	5,224.65
Rel	4,200.35
Irf7	4,080.12
Ass1	4,069.44
Eif2ak3	3,783.77
Oasl	3,774.34
Oas1a	3,735.38
Tspo	3,703.37
Gstt1	3,385.96
Atf3	3,226.96
Closeness centrality	
Nos3	0.04
Mmp9	0.04
Smad2	0.04
Prkar2b	0.04
Rel	0.04
Egr1	0.04
Eif2ak3	0.04
Hdac5	0.04
Atf3	0.04
Ass1	0.04
Snai2	0.04
Tspo	0.04
Rac2	0.04
Irf7	0.04
Mmp13	0.04

Table IV. Top five GO terms and pathways enriched for the nine key nodes.

Category	Term	P-value	Gene
GO	GO:0010033~response to organic substance	1.21E-04	*EGR1, PRKAR2B, MMP9, NOS3, SMAD2, EIF2AK3*
GO	GO:0048771~tissue remodeling	7.56E-04	*RAC2, MMP9, NOS3*
GO	GO:0044057~regulation of system process	9.23E-04	*EGR1, MMP9, NOS3, EIF2AK3*
GO	GO:0007242~intracellular signaling cascade	1.85E-03	*PRKAR2B, REL, RAC2, SMAD2, EIF2AK3*
GO	GO:0051969~regulation of transmission of nerve impulse	5.57E-03	*EGR1, MMP9, EIF2AK3*
PATHWAY	rno05200:Pathways in cancer	4.13E-02	*RAC2, MMP9, SMAD2*

GO, Gene Ontology.

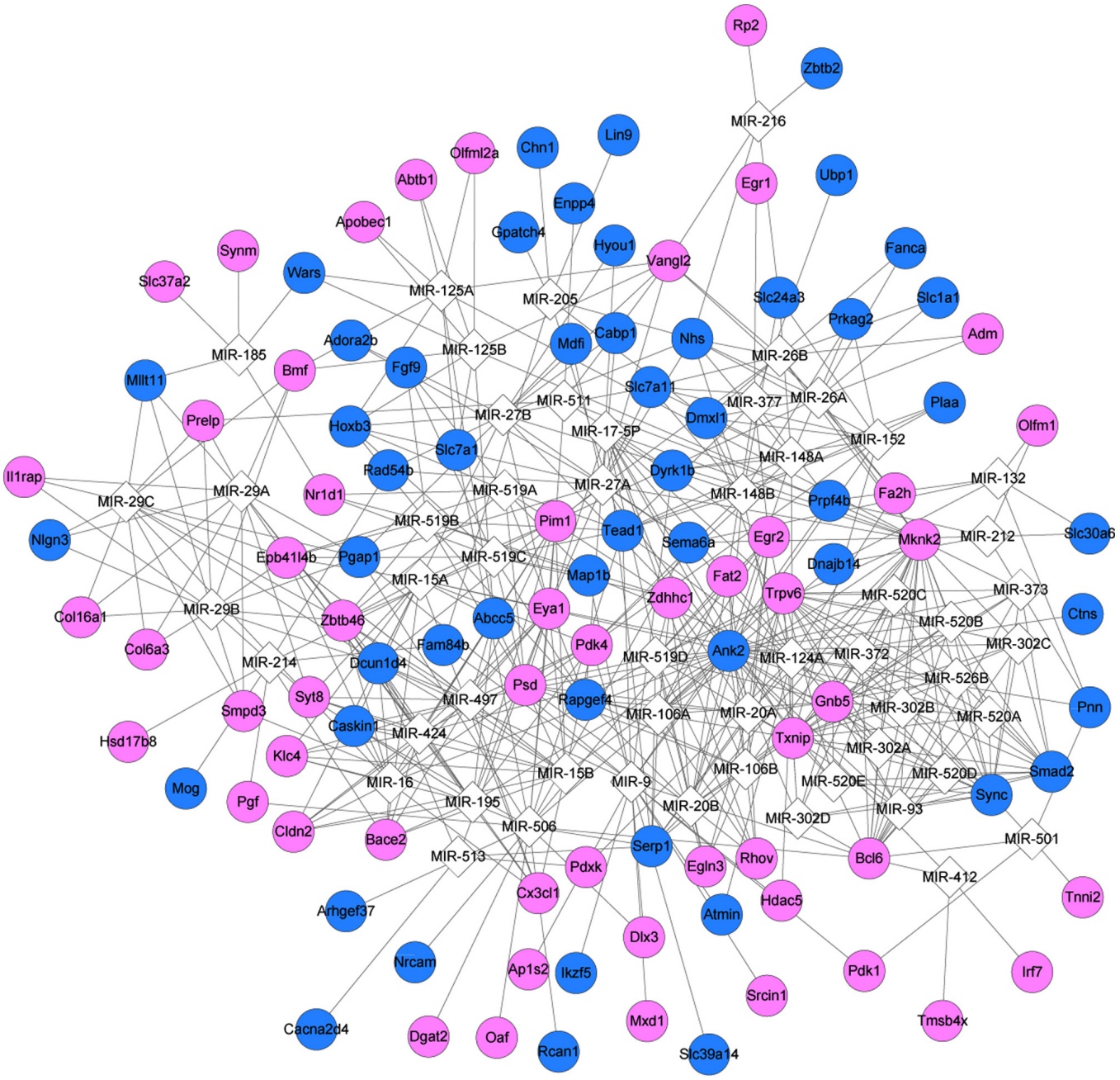

Figure 7. The miRNA-target regulatory network. Pink circles, blue circles, and white quadrangles represent upregulated genes, downregulated genes, and miRNAs, respectively. miRNA/miR, microRNA. Lines between nodes represent regulatory relationships.

Table V. Results of miRNA prediction.

miRNA	Adjusted P-value	Target
miR-506	0.0013	*Pgap1, Bcl6, Dlx3, Pim1, Eya1, Oaf, Tead1, Egr2, Smpd3, Pgf, Dnajb14, Dgat2, Caskin1, Slc7a1, Sema6a, Nrcam, Rcan1, Serp1, Arhgef37*
miR-27A, miR-27B	0.0013	*Adora2b, Pgap1, Mknk2, Vangl2, Slc7a11, Ank2, Hoxb3, Dcun1d4, Eya1, Nhs, Sema6a, Cabp1, Rad54b, Mdfi, Hyou1*
miR-148A, miR-152, miR-148B	0.0028	*Prkag2, Dmxl1, Pdk4, Slc7a11, Ank2, Dyrk1b, Nhs, Txnip, Plaa, Tead1, Slc24a3*
miR-205	0.0083	*Gpatch4, Tead1, Dmxl1, Lin9, Fam84b, Nhs, Chn1*
miR-124A	0.0083	*Map1b, Dmxl1, Hdac5, Fa2h, Eya1, Sema6a, Pdxk, Atmin, Tead1, Sync, Egr2, Serp1, Ctns, Pnn*
miR-26A		
miR-26B	0.0083	*Slc1a1, Dmxl1, Mknk2, Vangl2, Slc7a11, Pim1, Adm, Fa2h, Nhs, Fanca*
miR-29A, miR-29B		
miR-29C	0.0107	*Il1rap, Pgap1, Col6a3, Smpd3, Col16a1, Dcun1d4, Syt8, Prelp, Mllt11, Nlgn3, Epb41l4b, Bmf, Zbtb46*
miR-125B, miR-125A	0.0109	*Abcc5, Wars, Mknk2, Vangl2, Hoxb3, Slc7a1, Abtb1, Olfml2a, Apobec1, Bmf*
miR-15A, miR-16, miR-15B, miR-195, miR-424, miR-497	0.0111	*Abcc5, Cx3cl1, Cldn2, Pdk4, Klc4, Ank2, Dcun1d4, Pim1, Eya1, Caskin1, Syt8, Bace2, Epb41l4b, Zbtb46*
miR-9	0.0163	*Map1b, Pgap1, Pdk4, Hdac5, Bcl6, Ank2, Dlx3, Dcun1d4, Dyrk1b, Ikzf5, Slc39a14, Ap1s2*
miR-17-5P, miR-20A, miR-106A, miR-106B, miR-20B, miR-519D	0.0208	*Fat2, Trpv6, Mknk2, Psd, Ank2, Rapgef4, Zdhhc1, Txnip, Rhov, Egr2, Serp1, Gnb5, Egln3*
miR-412	0.0208	*Tmsb4x, Bcl6, Ank2, Irf7*
miR-212, miR-132	0.0232	*Sema6a, Prpf4b, Slc30a6, Olfm1, Dnajb14, Pnn*
miR-216	0.0232	*Zbtb2, Vangl2, Slc24a3, Rp2, Nhs*
miR-513	0.0338	*Pdxk, Cacna2d4, Serp1, Dcun1d4, Eya1*
miR-9	0.0338	*Mxd1, Tead1, Atmin, Prpf4b, Pdk1, Fam84b, Srcin1*
miR-214	0.0338	*Hsd17b8, Bace2, Mog, Rad54b, Pgf, Pim1, Fam84b*
miR-185	0.0338	*Mllt11, Wars, Nr1d1, Slc37a2, Synm*
miR-519C, miR-519B, miR-519A	0.0338	*Fgf9, Map1b, Nr1d1, Psd, Hoxb3, Rapgef4, Zdhhc1, Tead1, Epb41l4b, Zbtb46*
miR-501	0.0338	*Sync, Pdk1, Tnni2, Bcl6, Pnn*
miR-511	0.0472	*Prelp, Prpf4b, Enpp4, Vangl2, Dyrk1b, Eya1*
miR-93, miR-302A, miR-302B, miR-302C, miR-302D, miR-372, miR-373, miR-520E, miR-520A, miR-526B, miR-520B, miR-520C, miR-520D	0.0472	*Trpv6, Mknk2, Bcl6, Ank2, Smad2, Txnip, Sync, Gnb5*
miR-377	0.0473	*Fat2, Tead1, Prpf4b, Egr2, Ubp1, Egr1*

miR, microRNA.

In conclusion, *HNF-4α* contributes to the differentiation of WB-F344 cells into hepatocytes. *MMP9*, *EGR1*, *SMAD2* and *RAC2* may be targets of *HNF-4α* during the hepatic differentiation of WB-F344 cells. However, further experiments, including RT-qPCR analysis, are required to confirm the targets of *HNF-4α* in the hepatic differentiation of WB-F344 cells.

Acknowledgements

Not applicable.

Funding

No funding was received.

Availability of data and materials

The datasets generated and/or analyzed during the current study are available in the Sequence Read Archive database repository (http://www.ncbi.nlm.nih.gov/sra/) under accession no. SRP135721.

Authors' contributions

YS and BS contributed to the study design, DehZ and DerZ contributed to data collection, BW and DehZ contributed to data analysis and interpretation, YS conducted statistical analysis. All authors read and approved the final manuscript.

Ethics approval and consent to participate

Not applicable.

Patient consent for publication

Not applicable.

Competing interests

The authors declare that they have no competing interests.

References

1. Chandra V, Huang P, Potluri N, Wu D, Kim Y and Rastinejad F: Multidomain integration in the structure of the HNF-4α nuclear receptor complex. Nature 495: 394-398, 2013.
2. Saha SK, Parachoniak CA, Ghanta KS, Fitamant J, Ross KN, Najem MS, Gurumurthy S, Akbay EA, Sia D, Cornella H, *et al*: Mutant IDH inhibits HNF-4α to block hepatocyte differentiation and promote biliary cancer. Nature 513: 110-114, 2014.
3. Li J, Ning G and Duncan SA: Mammalian hepatocyte differentiation requires the transcription factor HNF-4α. Genes Dev 14: 464-474, 2000.
4. Takayama K, Inamura M, Kawabata K, Katayama K, Higuchi M, Tashiro K, Nonaka A, Sakurai F, Hayakawa T, Furue MK and Mizuguchi H: Efficient generation of functional hepatocytes from human embryonic stem cells and induced pluripotent stem cells by HNF4α transduction. Mol Ther 20: 127-137, 2012.
5. Chen KT, Pernelle K, Tsai YH, Wu YH, Hsieh JY, Liao KH, Guguen-Guillouzo C and Wang HW: Liver X receptor α (LXRα/NR1H3) regulates differentiation of hepatocyte-like cells via reciprocal regulation of HNF4α. J Hepatol 61: 1276-1286, 2014.
6. Simó R, Barbosa-Desongles A, Hernandez C and Selva DM: IL1β down-regulation of sex hormone-binding globulin production by decreasing HNF-4α via MEK-1/2 and JNK MAPK pathways. Mol Endocrinol 26: 1917-1927, 2012.
7. Simó R, Barbosadesongles A, Sáezlopez C, Lecube A, Hernandez C and Selva DM: Molecular mechanism of TNFα-induced down-regulation of SHBG expression. Mol Endocrinol 26: 438-446, 2012.
8. Li WQ, Li YM, Guo J, Liu YM, Yang XQ, Ge HJ, Xu Y, Liu HM, He J and Yu HY: Hepatocytic precursor (stem-like) WB-F344 cells reduce tumorigenicity of hepatoma CBRH-7919 cells via TGF-beta/Smad pathway. Oncol Rep 23: 1601-1607, 2010.
9. Liu J, Liu Y, Wang H, Hao H, Han Q, Shen J, Shi J, Li C, Mu Y and Han W: Direct differentiation of hepatic stem-like WB cells into insulin-producing cells using small molecules. Sci Rep 3: 1185, 2013.
10. Couchie D, Holic N, Chobert MN, Corlu A and Laperche Y: In vitro differentiation of WB-F344 rat liver epithelial cells into the biliary lineage. Differentiation 69: 209-215, 2002.
11. Yang Z, Wang L and Wang X: Matrine induces the hepatic differentiation of WB-F344 rat hepatic progenitor cells and inhibits Jagged 1/HES1 signaling. Mol Med Rep 14: 3841-3847, 2016.
12. Vasilescu C, Rossi S, Shimizu M, Tudor S, Veronese A, Ferracin M, Nicoloso MS, Barbarotto E, Popa M, Stanciulea O, *et al*: MicroRNA fingerprints identify miR-150 as a plasma prognostic marker in patients with sepsis. PLoS One 4: e7405, 2009.
13. Yao H, Jia Y, Zhou J, Wang J, Li Y, Wang Y, Yue W and Pei X: RhoA promotes differentiation of WB-F344 cells into the biliary lineage. Differentiation 77: 154-161, 2009.
14. Zhang Y, Li XM, Zhang FK and Wang BE: Activation of canonical Wnt signaling pathway promotes proliferation and self-renewal of rat hepatic oval cell line WB-F344 in vitro. World J Gastroenterol 14: 6673-6680, 2008.
15. Arocho A, Chen B, Ladanyi M and Pan Q: Validation of the 2-DeltaDeltaCt calculation as an alternate method of data analysis for quantitative PCR of BCR-ABL P210 transcripts. Diagn Mol Pathol 15: 56-61, 2006.
16. Kim D, Pertea G, Trapnell C, Pimentel H, Kelley R and Salzberg SL: TopHat2: Accurate alignment of transcriptomes in the presence of insertions, deletions and gene fusions. Genome Biol 14: R36, 2014.
17. Strozzi F and Aerts J: A Ruby API to query the Ensembl database for genomic features. Bioinformatics 27: 1013-1014, 2011.
18. Anders S, Pyl PT and Huber W: HTSeq-a Python framework to work with high-throughput sequencing data. Bioinformatics 31: 166-169, 2015.
19. Nikolayeva O and Robinson MD: edgeR for differential RNA-seq and ChIP-seq analysis: An application to stem cell biology. Methods Mol Biol 1150: 45-79, 2014.
20. Robinson MD, Mccarthy DJ and Smyth GK: edgeR: A Bioconductor package for differential expression analysis of digital gene expression data. Bioinformatics 26: 139-140, 2010.
21. Law CW, Chen Y, Shi W and Smyth GK: voom: Precision weights unlock linear model analysis tools for RNA-seq read counts. Genome Biol 15: R29, 2014.
22. Ritchie ME, Phipson B, Wu D, Hu Y, Law CW, Shi W and Smyth GK: limma powers differential expression analyses for RNA-sequencing and microarray studies. Nucleic Acids Res 43: e47, 2015.
23. Yu L, Gulati P, Fernandez S, Pennell M, Kirschner L and Jarjoura D: Fully moderated T-statistic for small sample size gene expression arrays. Stat Appl Genet Mol Biol 10: 1-22, 2011.
24. Huang DW, Sherman BT and Lempicki RA: Systematic and integrative analysis of large gene lists using DAVID bioinformatics resources. Nat Protoc 4: 44-57, 2009.
25. Gene Ontology Consortium: Gene Ontology Consortium: Going forward. Nucleic Acids Res 43 (Database Issue): D1049-D1056, 2015.
26. Kanehisa M, Sato Y, Kawashima M, Furumichi M and Tanabe M: KEGG as a reference resource for gene and protein annotation. Nucleic Acids Res 44: D457-D462, 2016.
27. Franceschini A, Szklarczyk D, Frankild S, Kuhn M, Simonovic M, Roth A, Lin J, Minguez P, Bork P, von Mering C and Jensen LJ: STRING v9.1: Protein-protein interaction networks, with increased coverage and integration. Nucleic Acids Res 41 (Database Issue): D808-D815, 2013.
28. Saito R, Smoot ME, Ono K, Ruscheinski J, Wang PL, Lotia S, Pico AR, Bader GD and Ideker T: A travel guide to Cytoscape plugins. Nat Methods 9: 1069-1076, 2012.
29. Tang Y, Li M, Wang J, Pan Y and Wu FX: CytoNCA: A cytoscape plugin for centrality analysis and evaluation of protein interaction networks. Biosystems 127: 67-72, 2015.
30. Rito T, Deane CM and Reinert G: The importance of age and high degree, in protein-protein interaction networks. J Comput Biol 19: 785-795, 2012.
31. Goh KI, Oh E, Kahng B and Kim D: Betweenness centrality correlation in social networks. Phys Rev E Stat Nonlin Soft Matter Phys 67: 017101, 2003.
32. Okamoto K, Chen W and Li XY: Ranking of closeness centrality for large-scale social networks. International Workshop on Frontiers in Algorithmics. Front Algorithmics: 186-195, 2008.
33. Wang J, Duncan D, Shi Z and Zhang B: WEB-based GEne SeT analysis toolkit (WebGestalt): Update 2013. Nucleic Acids Res 41: W77-W83, 2013.
34. Khurana S, Jaiswal AK and Mukhopadhyay A: Hepatocyte nuclear factor-4α induces transdifferentiation of hematopoietic cells into hepatocytes. J Biol Chem 285: 4725-4731, 2010.
35. Walesky C and Apte U: Role of hepatocyte nuclear factor 4α (HNF4α) in cell proliferation and cancer. Gene Expr 16: 101-108, 2015.

36. Kimata T, Nagaki M, Tsukada Y, Ogiso T and Moriwaki H: Hepatocyte nuclear factor-4alpha and -1 small interfering RNA inhibits hepatocyte differentiation induced by extracellular matrix. Hepatol Res 35: 3-9, 2006.
37. Garibaldi F, Cicchini C, Conigliaro A, Santangelo L, Cozzolino AM, Grassi G, Marchetti A, Tripodi M and Amicone L: An epistatic mini-circuitry between the transcription factors Snail and HNF4α controls liver stem cell and hepatocyte features exhorting opposite regulation on stemness-inhibiting microRNAs. Cell Death Differ 19: 937-946, 2012.
38. Walesky C, Gunewardena S, Terwilliger EF, Edwards G, Borude P and Apte U: Hepatocyte-specific deletion of hepatocyte nuclear factor-4α in adult mice results in increased hepatocyte proliferation. Am J Physiol Gastrointest Liver Physiol 304: G26-G37, 2013.
39. Kim TH, Mars WM, Stolz DB and Michalopoulos GK: Expression and activation of pro-MMP-2 and pro-MMP-9 during rat liver regeneration. Hepatology 31: 75-82, 2000.
40. Pham Van T, Couchie D, Martin-Garcia N, Laperche Y, Zafrani ES and Mavier P: Expression of matrix metalloproteinase-2 and -9 and of tissue inhibitor of matrix metalloproteinase-1 in liver regeneration from oval cells in rat. Matrix Biol 27: 674-681, 2008.
41. Han YP, Yan C, Zhou L, Qin L and Tsukamoto H: A matrix metalloproteinase-9 activation cascade by hepatic stellate cells in trans-differentiation in the three-dimensional extracellular matrix. J Biol Chem 282: 12928-12939, 2007.
42. Kollet O, Shivtiel S, Chen YQ, Suriawinata J, Thung SN, Dabeva MD, Kahn J, Spiegel A, Dar A, Samira S, *et al*: HGF, SDF-1, and MMP-9 are involved in stress-induced human $CD34^+$ stem cell recruitment to the liver. J Clin Invest 112: 160-169, 2003.
43. Kim HL, Cha JH, Park NR, Bae SH, Choi JY and Yoon SK: 304 EGR1 promotes the differentiation of bm-derived mesenchymal stem cells into functional hepatocyte with mesenchymal-to-epithelial transition. J Hepatol 58: S128, 2013.
44. Zhang Y, Bonzo JA, Gonzalez FJ and Wang L: Diurnal regulation of the early growth response 1 (Egr-1) protein expression by hepatocyte nuclear factor 4alpha (HNF4alpha) and small heterodimer partner (SHP) cross-talk in liver fibrosis. J Biol Chem 286: 29635-29643, 2011.
45. Ju W, Ogawa A, Heyer J, Nierhof D, Yu L, Kucherlapati R, Shafritz DA and Böttinger EP: Deletion of Smad2 in mouse liver reveals novel functions in hepatocyte growth and differentiation. Mol Cell Biol 26: 654-667, 2006.
46. Jiang F, Mu J, Wang X, Ye X, Si L, Ning S, Li Z and Li Y: The repressive effect of miR-148a on TGF beta-SMADs signal pathway is involved in the glabridin-induced inhibition of the cancer stem cells-like properties in hepatocellular carcinoma cells. PLoS One 9: e96698, 2014.
47. Teng NY, Liu YS, Wu HH, Liu YA, Ho JH and Lee OK: Promotion of mesenchymal-to-epithelial transition by Rac1 inhibition with small molecules accelerates hepatic differentiation of mesenchymal stromal cells. Tissue Eng Part A 21: 1444-1454, 2015.